Macromolecular Research

Article

DOI 10.1007/s13233-019-7072-x

www.springer.com/13233 pISSN 1598-5032 eISSN 2092-7673

Interpenetrating Polymer Network Hydrogels of Gelatin and Poly(ethylene glycol) as an Engineered 3D Tumor Microenvironment

Dong Shin Lee[2]
Jeon Il Kang[2]
Byeong Hee Hwang*[,1,2]
Kyung Min Park*[,1,2]

[1] Division of Bioengineering, College of Life Sciences and Bioengineering, Incheon National University, 119 Academy-ro, Yeonsu-gu, Incheon 22012, Korea
[2] Department of Bioengineering and Nano-Bioengineering, Incheon National University, 119 Academy-ro, Yeonsu-gu, Incheon 22012, Korea

Received September 17, 2018 / Revised October 29, 2018 / Accepted November 1, 2018

Abstract: An emerging trend in cancer research is to develop engineered tumor models using bio-inspired biomaterials that can mimic the native tumor microenvironment. Although various bio-inspired hydrogels have been utilized, it is still challenging to develop advanced polymeric hydrogel materials that can more accurately reconstruct critical aspects of the native tumor microenvironment. Herein, we present interpenetrating polymer network (IPN) hydrogels composed of thiolated gelatin and tyramine-conjugated poly(ethylene glycol), which form IPN hydrogels *via* horseradish peroxidase-mediated dual cross-linking reactions. We demonstrate that the IPN hydrogels exhibit independently controllable physicochemical properties. Also, the IPN hydrogels show resistance to the proteolytic enzymes and cytocompatibility for long-term culture of human fibrosarcoma (HT1080) cells. Moreover, we utilize the engineered tumor construct as a platform to evaluate the effect of matrix stiffness on cancer cell proliferation and drug resistance against the anticancer drug 5-fluorouracil as a model drug. In conclusion, we suggest that our IPN hydrogel is a promising material to study cancer biology and to screen innovative therapeutic agents for better clinical outcomes.

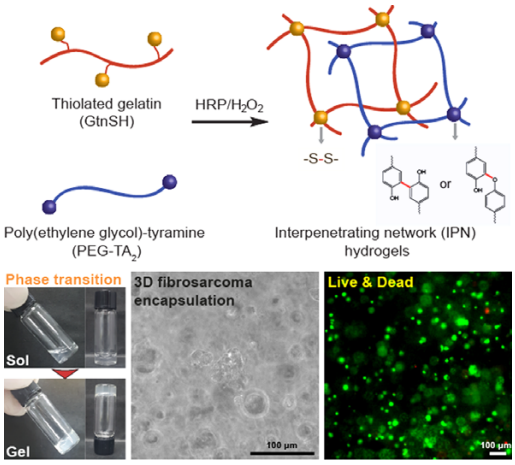

Keywords: polymeric hydrogels, injectable hydrogels, engineered tumor models, tumor microenvironments, drug resistance.

1. Introduction

Despite advances in medical technology, cancer is a destructive disease that is a leading cause of death worldwide.[1,2] Although many new drugs are being developed for chemotherapies, the therapeutics result in high failure rates because current preclinical models (*e.g., in vitro* and *in vivo* animal models) cannot accurately predict their efficacy in clinical trials.[3] Therefore, the development of preclinical models that precisely predict clinical outcomes remains a challenge for cancer treatment. To develop advanced preclinical models, we need to better understand the native tumor microenvironment, which has been implicated as a crucial factor in the process of cancer development and metastasis.[4,5] Native tumor environments present pathological conditions, including abnormal extracellular matrix remodeling, tumor-associated angiogenesis, and pressure of tumor mass.[6-8] Growing evidence has demonstrated that these parameters play critical roles in regulating cancer progression and metastasis. Thus, an emerging trend in cancer research is the design of engineered tumor models using bio-inspired biomaterials that can precisely recapitulate the native tumor microenvironment.

In advanced biomaterials engineering, various bio-inspired biomaterials have been utilized as artificial cellular microenvironments to reconstruct the native tumor microenvironment for cancer research. Among these, polymeric hydrogels are promising materials to create engineered tumor constructs owing to their tunable properties and their structural similarity to native tumors.[9,10] The most basic requirements for the development of artificial tumor models using polymeric hydrogels are 1) adequate phase transition time to homogeneously encapsulate cells within the matrices, 2) cytocompatibility to support cancer cell growth, 3) hydrogel stability for long-term cell culture, and 4) independently adjustable physicochemical properties. Although various types of hydrogel materials have been used to create engineered tumor constructs, the development of advanced polymeric hydrogel materials with desired properties to recapitulate critical aspects of the native tumor microenvironment remains a challenge.

Herein, we report a new type of interpenetrating polymer network (IPN) hydrogel composed of gelatin and poly(ethylene glycol) (PEG), which can provide an engineered three-dimensional (3D) tumor microenvironment. The IPN hydrogels are formed *via* horseradish peroxidase-mediated dual cross-linking reaction between thiolated gelatin and tyramine-conjugated PEG moieties. They show independently controllable gelation time and

Acknowledgments: This work was supported by the Incheon National University International Cooperative Research Grants in 2016.

***Corresponding Authors:** Byeong Hee Hwang (bhwang@inu.ac.kr), Kyung Min Park (kmpark@inu.ac.kr)

tunable mechanical properties. The IPN hydrogels exhibit resistance to the proteolytic enzymes and cytocompatibility for long-term cancer cell culture. Moreover, we utilize the engineered tumor model as a platform to study the effect of matrix stiffness on cancer cell activity and drug resistance. We suggest that our IPN hydrogel is a promising material to create engineered tumor microenvironments for studying basic cancer biology and screening newly developed anticancer drugs.

2. Experimental

2.1. Materials

For polymer synthesis and hydrogel fabrication, gelatin (Gtn, type A from porcine skin, less than 300 bloom), 2-iminothiolane hydrochloride (Traut's reagent, TR), dimethyl sulfoxide (DMSO, anhydrous), deuterium oxide (D_2O), poly(ethylene glycol) (PEG, average M_n=4,000, platelets), 4-(dimethyl amino) pyridine (DMAP), tyramine (TA), dichloromethane (MC, anhydrous), *p*-nitrophenyl chloroformate (PNC), horseradish peroxidase (HRP, type VI, salt-free, 250-330 units per milligram, solid), hydrogen peroxide (H_2O_2, 30 w/v% in H_2O), chloroform-d ($CDCl_3$), and collagenase from *Clostridium histolyticum* type II were purchased from Sigma-Aldrich (St. Louis, MO). Triethylamine (TEA) was obtained from Kanto Chemical Co. (Chuo-ku, Tokyo). Ethyl ether was purchased from Samchun Pure Chemical (Gangnam, Seoul). Dialysis membrane (molecular weight cut-off=3,500 Da) was purchased from Spectrum Laboratories (Rancho Dominiguez, CA). Hydrochloric acid standard solution (1 N) was purchased from Daejung (Siheung, Gyeonggi). 5,5'-dithio-bis-(2-nitrobenzoic acid) (Ellman's reagent) was purchased from Thermo Scientific (Rockford, IL).

For *in vitro* cell culture, human fibrosarcoma (HT1080) cells were obtained from the Korean Cell Line Bank (Jongno, Seoul). Dulbecco's phosphate-buffered saline (DPBS), Dulbecco's modified Eagle's medium (DMEM), newborn calf serum (NBCS), penicillin streptomycin (P/S), and 0.25% trypsin-EDTA were purchased from Gibco (Grand Island, NY). Live/dead kit was obtained from Molecular Probes (Eugene, OR). WST-1 cell proliferation kit was purchased from Roche (Grenzacherstrasse, Basel). 5-Fluorouracil (5-FU) was obtained from Sigma-Aldrich (St. Louis, MO).

2.2. Synthesis and characterization of thiolated gelatin (GtnSH) and tyramine-conjugated PEG (PEG-TA_2)

Thiolated gelatin (GtnSH) was synthesized using TR as previously reported.[11] Gtn (500 mg) was dissolved in 50 mL of anhydrous DMSO at 40 °C under nitrogen (N_2) atmosphere. TR (50 mg, 0.36 mmol) was dissolved in 5 mL of anhydrous DMSO. The TR solution was then applied to the Gtn solution, and the reaction was conducted at 40 °C for 24 h under N_2 atmosphere. After the conjugative reaction, the solution was dialyzed against 5 mM HCl solution for 48 h and then against 1 mM HCl solution for 24 h (molecular weight cut-off=3,500 Da) to remove unconjugated TR molecules. After dialysis, the GtnSH polymer was obtained by freeze-drying and the product was kept in a dry keeper before use. The chemical structure of the polymer was characterized using a proton nuclear magnetic resonance (^{1}H NMR) spectrometer (Agilent 400-MR, Agilent Technologies, CA). For ^{1}H NMR measurement, we prepared GtnSH solutions in 10 mg/mL D_2O. The thiol content in the polymer was determined by Ellman's assay according to the manufacturer's instructions. The GtnSH solution (100 μL, 1 mg/mL in deionized water) was mixed with Ellman's reagent (100 μL). After 20 min of incubation at 25 °C, we measured the absorbance at 405 nm using ultraviolet spectrophotometry (Multiskan EX, Thermo Scientific, Rockford, IL). The thiol content was determined using a calibration curve obtained by monitoring the absorbance of known concentrations of cysteine (0.0025-0.05 mg/mL) and is expressed as μmol of free thiol groups per gram of GtnSH polymer.

PEG-TA_2 was synthesized by a two-step reaction as previously reported.[12] We first synthesized amine-reactive PEG by conjugating PNC molecules to the terminal hydroxyl groups of PEG. Briefly, PEG (2.0 g, 0.5 mmol) was dissolved in 40 mL of anhydrous MC and reacted with DMAP (183.3 mg, 1.5 mmol) and TEA (209.2 μL, 1.5 mmol) at 25 °C for 15 min to activate the terminal hydroxyl groups of PEG. The activated PEG solution was applied to PNC (302.3 mg, 1.5 mmol) dissolved in 30 mL of anhydrous MC by the dropping method. The reaction was conducted at 4 °C for 24 h under N_2 atmosphere. After conjugative reaction, the polymer solution was concentrated using a rotary evaporator (Rotavapor R-215, BUCHI) at 40 °C, followed by precipitation in cold ethyl ether. The product was kept in a vacuum oven to remove the solvent, yielding a white powder of the PEG-PNC_2 conjugate. The chemical structure and conjugation efficiency of PNC was determined by ^{1}H NMR. For the ^{1}H NMR measurements, the polymers were dissolved in $CDCl_3$ (10 mg/mL).

To synthesize PEG-TA_2, PEG-PNC_2 (2.0 g, 0.5 mmol) was dissolved in 40 mL of DMSO at 25 °C. TA solution (205.8 mg, 1.5 mmol) dissolved in 2 mL of DMSO was mixed with the PEG-PNC_2 solution. The conjugative reaction was conducted at 25 °C for 24 h and the solutions was purified by dialysis against distilled water for three days. The polymer powder was obtained by lyophilization and stored in a dry keeper before use. The chemical structures and degree of substitution of TA were characterized by ^{1}H NMR spectroscopy. For the ^{1}H NMR measurement, the polymer was dissolved in D_2O (10 mg/mL).

2.3. Preparation of IPN hydrogels

IPN hydrogels were prepared by a simple mixture of the polymer, HRP, and H_2O_2 solutions. To fabricate 100 μL of IPN hydrogels, 80 μL of polymer solution (final concentrations of PEG-TA_2: 0.5-3 wt% and GtnSH: 0-2 wt%), 10 μL of HRP (0.087-1.375 U/mL), and 10 μL of H_2O_2 (1.25-7.5 mM) were mixed and gently shaken. All solutions were prepared in DPBS.

2.4. Measurement of gelation time and rheological analysis

The phase transition time of IPN hydrogels was determined by the vial tilting method as previously reported.[13,14] The hydrogels (100 μL) were prepared in 1.5-mL microtubes and mixed gently. The gelation time was determined as the time point at which no flow was observed after inverting the solution. The gelation

time was measured with different concentrations of polymer, HRP, and H_2O_2.

The elastic modulus (G') of the IPN hydrogels was measured using a rheometer (DHR-1, TA instruments, New Castle, DE) with parallel plates (diameter, 20 mm) and a gap of 600 μm in oscillatory mode with a frequency of 0.1 Hz and strain of 0.1% at 37 °C. For the rheological experiment, the hydrogels (200 μL) were prepared on the plate in the instrument. We performed dynamic time sweep on the hydrogel samples in various conditions depending on the polymer, HRP, and H_2O_2 concentrations (final concentrations of GtnSH, 0-2.0 wt%; PEG-TA_2, 0.5-2.0 wt%; HRP, 0.087-1.375 U/mL; H_2O_2, 2.5-8.0 mM). We also monitored the G' of the IPN hydrogels encapsulating HT1080 cancer cells (2.0×10^6 cells/mL) at the same conditions.

2.5. *In vitro* proteolytic degradation study

In vitro proteolytic degradation of the IPN hydrogels was determined by the gravimetrical method using collagenase type II, as previously reported.[15] Hydrogels (100 μL) were prepared in 1.5-mL microtubes and incubated in 200 μL of DPBS with or without collagenase (0.01 mg/mL) at 37 °C. At the pre-determined time points, the medium was removed from the microtubes and the weight of the hydrogels (W_d) was measured, followed by addition of fresh medium. The weight of the remaining hydrogels was then calculated according to the following equation: Weight of hydrogel (%)=(W_d/W_i)×100%; where W_d is the weight of the remaining hydrogel and W_i is the weight of the initial hydrogel.

2.6. Three-dimensional (3D) encapsulation of human fibrous sarcoma (HT1080)

For 3D cell culture, all solutions dissolved in DPBS were sterilized by filtration using a syringe filter with a pore size of 200 nm. The polymer solutions (GtnSH, 2 wt%; PEG-TA_2, 2 wt%) were mixed with HT1080 cells to create a cell suspension (2.0×10^6 cells/mL), and HRP (1.375 U/mL) and H_2O_2 (6.0-8.0 mM) were added at a volume ratio of 8:1:1 (polymer solution/HRP/H_2O_2). The mixture (60 μL) was placed in a cylindrical mold (diameter= 5 mm; thickness=1 mm) and allowed to form a hydrogel at 25 °C. The hydrogel discs encapsulating cells were placed in a 48-well plate and cultured with 500 μL of culture medium (high-glucose DMEM, 10% NBCS, and 1% P/S) under standard culture condition (37 °C and 5% of CO_2) for up to seven days. The cell morphology was observed using optical microscopy (inverted phase-contrast microscope, Eclipse TS100, Nikon). To assess cell viability, the hydrogels were treated with 200 μL of DPBS containing 2 μM acetomethoxy derivate of calcein and 4 μM ethidium homodimer-1 after three and seven days of culture and incubated for 30 min. The stained samples were washed with DPBS and observed using fluorescence microscopy (inverted microscope, Eclipse Ti-E system, Nikon). For quantitative cell proliferation analysis, WST-1 assay was performed according to the manufacturer's instruction. Briefly, hydrogels encapsulating cells were incubated in 150 μL of culture medium containing 10% WST-1 solution for 10 min. Then, 100 μL of the medium was placed into a 96-well plate and the optical density was measured at a wavelength of 450 nm using a microplate reader.

2.7. Drug resistance test using anticancer drug (5-FU)

For 2D drug resistance study, HT1080 cells were seeded on 96-well plates (5×10^3 cells/well) and after 24 h, the cells were treated with 5-FU (0, 0.01, 0.1, 1, 5, and 10 mg/mL) and further incubated for 24 h. For 3D drug resistance testing, HT1080 cells cultured within hydrogels (final concentrations of GtnSH, 2 wt%; PEG-TA_2, 2 wt%; HRP, 1.375 U/mL; H_2O_2, 6.0-8.0 mM) were treated with the same doses of 5-FU. Cell viability was evaluated using the WST-1 assay and IC50 values were calculated from the non-linear dose-response curves using GraphPad Prism 5 (GraphPad Software Inc., La Jolla, CA).

2.8. Statistical analysis

Cell proliferation and drug resistance were evaluated using quadruplicate samples for each data point. Statistical analyses were carried out using GraphPad Prism 5. Two-tail *t*-test was used to determine the significance between each group. Significant levels were set at $^*P<0.05$, $^{**}P<0.01$, and $^{***}P<0.001$.

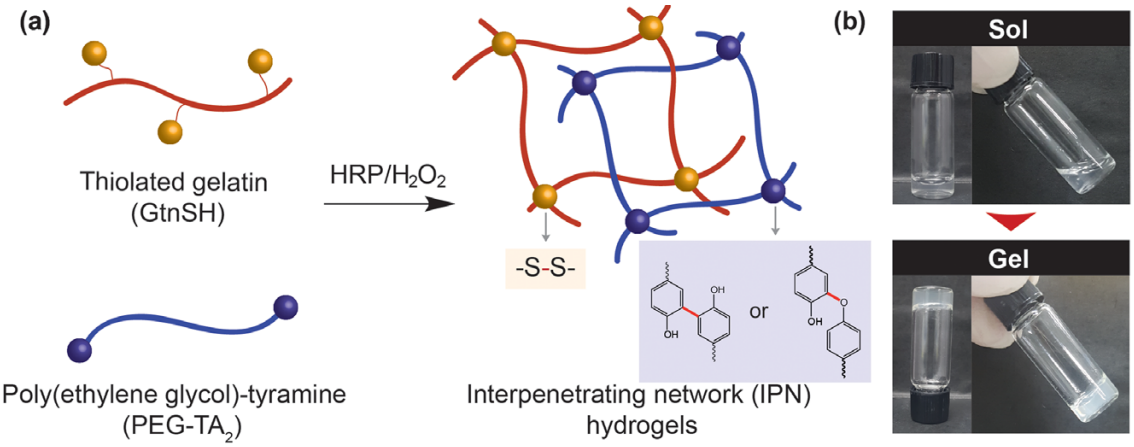

Figure 1. Interpenetrating polymer network (IPN) formation. (a) Schematic representation of IPN hydrogel formation in the HRP-mediated dual cross-linking reaction. (b) Digital images of the phase transition of the hydrogels.

3. Results and discussion

3.1. IPN hydrogel formation with controllable gelation time

GtnSH and PEG-TA_2 were synthesized as previously reported.[11,12,15] We hypothesized that GtnSH and PEG-TA_2 conjugates could form IPN hydrogels *via* HRP-mediated oxidative cross-linking reaction. In this reaction, HRP catalyzes di-tyramine formation *via* a carbon-oxygen bond between carbon at the ortho position and phenoxy oxygen, and disulfide bonds between thiyl radicals formed by radical transfer from the phenoxy radical, which result in IPN hydrogels composed of gelatin and PEG as polymer backbones (Figure 1(a)). We observed the opaque hydrogels owing to the semi-crystalline formation of GtnSH polymer backbone *via* disulfide bond during hydrogel formation (Figure 1(b)).[16,17] We selected gelatin as a bioactive polymer chain for its cellular activities, including cell-adhesive sites and proteolytic degradable moieties, which are crucial parameters in designing artificial cellular microenvironments.[18] We also chose PEG as another polymer backbone because of its hydrophilicity and non-proteolytic degradability.[19,20] In this way, the gelatin would regulate cellular activities while the PEG would provide a stable structural frame to support cell growth within the IPN hydrogels.

For 3D cell encapsulation within hydrogels, phase transition time is one of the most critical factors. Fast gelation time (<10 s) is inadequate for uniform cell encapsulation, whereas slow gelation time (>5 min) causes the cells to sink to the bottom because of gravity. We investigated the effect of hydrogel composition on the IPN hydrogel formation time. Toward this end, we measured the phase transition time depending on the concentrations of the polymer (GtnSH, 0-2.0 wt%; PEG-TA_2, 0.5-2.0 wt%), HRP (0.173-1.375 U/mL), and H_2O_2 (1.25-7.0 mM) solutions. The hydrogels showed controllable gelation time, ranging from 30 s to 6 min. As the PEG-TA_2 and HRP concentrations increased, the phase transition time decreased (PEG-TA_2, from 51 s to 30 s; HRP, from 343 s to 67 s) (Figure 2(a) and 2(c)). This result can be explained by the fact that the increased concentrations of PEG-TA_2 and HRP induced rapid 3D hydrogel network formation by facilitating the phenoxy radical.[12] H_2O_2 plays a critical role as a substrate in the HRP-mediated cross-linking reaction. Many studies have demonstrated that increased H_2O_2 concentrations induced faster hydrogel formation, but excess H_2O_2 may reduce the kinetics of hydrogel formation by inhibiting the enzymatic activity of HRP. We found that there were no significant differences in phase transition time above 5.5 mM H_2O_2, suggesting that the H_2O_2 concentration (from 5.5 mM to 7.0 mM) was saturated in this cross-linking reaction (Figure 2(d)). Interestingly, we noticed that increasing GtnSH content induced slower hydrogel formation, ranging from 62 s to 133 s (Figure 2(b)). This phenomenon occurred because the enzymatic activity of HRP was inhibited by the free thiol groups that could induce a structural deformation of the enzyme by the thiol exchange reaction.[21,22] Based on the results, we optimized the hydrogel composition with adequate gelation time (60-90 s) for the 3D cell studies.

In summary, we fabricated IPN hydrogels composed of gelatin and PEG through the HRP-mediated dual cross-linking reaction with controllable gelation time dependent on the hydrogel composition. This unique property is an advantage of the IPN hydrogels, as the easy fabrication and controllable gelation time allow the homogeneous encapsulation of target cells within the hydrogel matrices to create an engineered tumor construct.

3.2. Resistance of hydrogel matrices to proteolytic enzymes

Cancer cells overexpress and secrete proteases, which are capable of remodeling the native tumor microenvironments, thus facilitating tumor migration and metastasis.[23,24] Among the degradable enzymes, matrix metalloproteinases including collagenase have been implicated as a critical factor in tumor invasion and metastasis.[25-27] Therefore, resistance to proteolytic enzymes is one of the crucial parameter to consider when designing an artificial tumor model using hydrogel materials for long-term culture of either cancer cells or tumor tissues. We hypothesized that our IPN hydrogels composed of gelatin and PEG moieties could act as long-term stable matrices for creating engineered tumor microenvironments. Toward this, we examined the protease-sensitive degradation of the IPN hydrogels using collagenase. While the hydrogel composed solely of gelatin was decomposed entirely within five days, the IPN hydrogels retained 20-25% of their weight even after 30 days (Figure 3). We also noticed that increasing polymer content increased the hydrogel weight. For example, the weight of the IPN hydrogel with lower polymer contents (P1G1, 1% PEG-TA_2 and 1% GtnSH) was 39-76% of its original weight on day 7. Meanwhile, the weight of the hydrogel with higher concentrations (P2G2, 2% PEG-TA_2 and 2% GtnSH) was

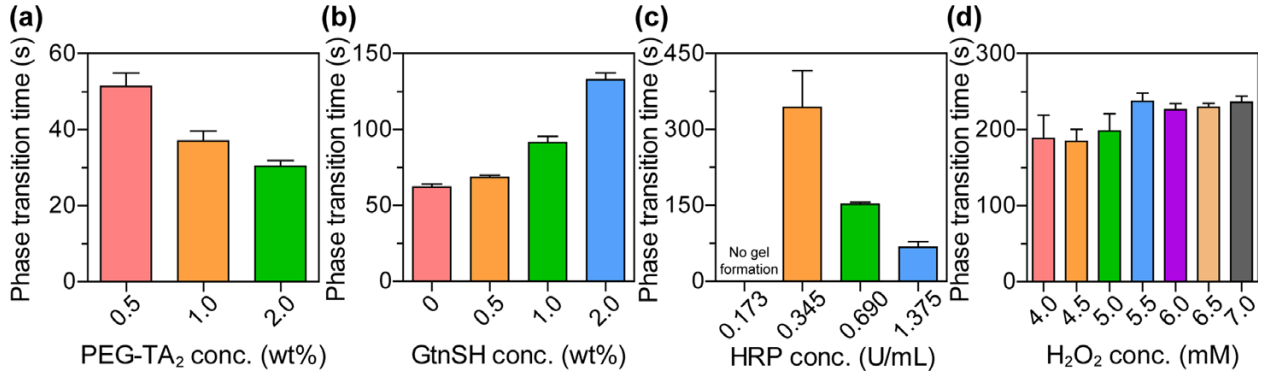

Figure 2. Controllable gelation time. The effect of the concentration of (a) PEG-TA_2, (b) GtnSH, (c) HRP, and (d) H_2O_2 on hydrogel formation kinetics.

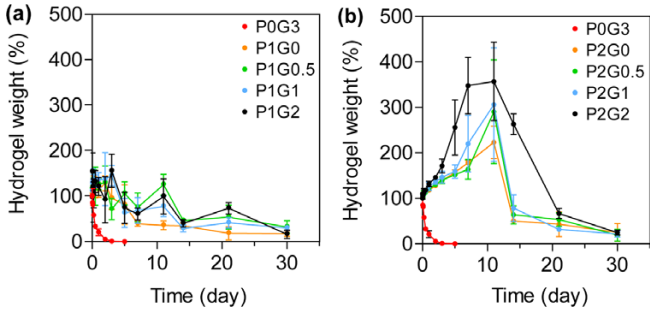

Figure 3. IPN hydrogel matrices with resistance to proteolytic enzymes. The effect of polymer composition on hydrogel weight: (a) 1 wt% PEG-TA_2 and (b) 2 wt% PEG-TA_2 with different GtnSH contents. Results are shown as the average ± s.d. (n=5).

178-348% of its original weight at the same time point. This result can be explained by the fact that higher concentrations of hydrophilic polymers (*e.g.* PEG and gelatin) can absorb more water during hydrogel degradation, which is consistent with previous reports.[15] Taken together, we demonstrated that our IPN hydrogels have resistance to the proteolytic enzyme, suggesting that the matrices may provide an artificial tumor microenvironment for long-term culture of cancer cells or tumor tissues.

3.3. Controllable matrix stiffness of the IPN hydrogels

Accumulating evidence has demonstrated that matrix stiffness is a crucial factor in cancer progression and metastasis.[28-30] We next speculated whether the IPN hydrogel could create 3D engineered tumor constructs with tunable matrix rigidity. To evaluate the elastic modulus (G'), we performed rheological analysis involving a dynamic time sweep of the hydrogels with varying PEG-TA_2, HRP, GtnSH, and H_2O_2 concentrations. Figure 4 exhibits the G' profiles of the IPN hydrogels with different compositions. The G' values increased as the concentrations of PEG-TA_2, HRP, and H_2O_2 increased because of the increase in cross-linking density. In the case of H_2O_2, hydrogels formed with H_2O_2 concentrations of greater than 6.0 mM showed similar elastic properties owing to the saturation of H_2O_2 for hydrogel formation. Interestingly, we noticed that higher GtnSH contents induced softer matrices because of the reduced HRP activities during hydrogel formation. These results demonstrated that G' varies with the hydrogel composition (PEG-TA_2, 0.01-810 Pa; GtnSH, 5-900 Pa; HRP, 0.03-1000 Pa; H_2O_2, 2-3800 Pa).

To investigate the effect of cell encapsulation on the hydrogel stiffness, we measured the G' values of the IPN hydrogels (PEG-TA_2, 2 wt%; GtnSH, 2 wt%; HRP, 1.375 U/mL) encapsulating HT1080 cells (2×10^6 cells/mL). We controlled the matrix stiffness by varying the concentration of H_2O_2. The elastic modulus was similar (2400-2700 Pa) in the IPN hydrogels without cells because the amount of H_2O_2 was saturated for hydrogel formation. Interestingly, the G' values decreased dramatically when cells were encapsulated within the IPN hydrogel matrices (Figure 4(e)). This result may be caused by the reduced crosslinking density as the cells may impede 3D network formation,[31] scavenge H_2O_2,[32,33] and inhibit enzyme activity[21,22] during hydrogel formation. Based on these results, we selected the optimized hydrogel matrices with different matrix stiffness (High, 8 mM H_2O_2; Medium, 7 mM H_2O_2; Low, 6 mM H_2O_2) for *in vitro* cell study. It should be noticed that the matrix stiffness of the cell-encapsulating hydrogels can be independently controlled by varying H_2O_2 without changing the polymer concentrations.

3.4. Engineered tumor models using IPN hydrogels

We utilized the IPN hydrogels as a platform to study the proliferative activities of cancer cells and to test their resistance against commercially available anticancer drugs. To create engineered tumor constructs, we encapsulated HT1080 cells into the optimized hydrogel matrices with varying stiffness (High, 1300 Pa;

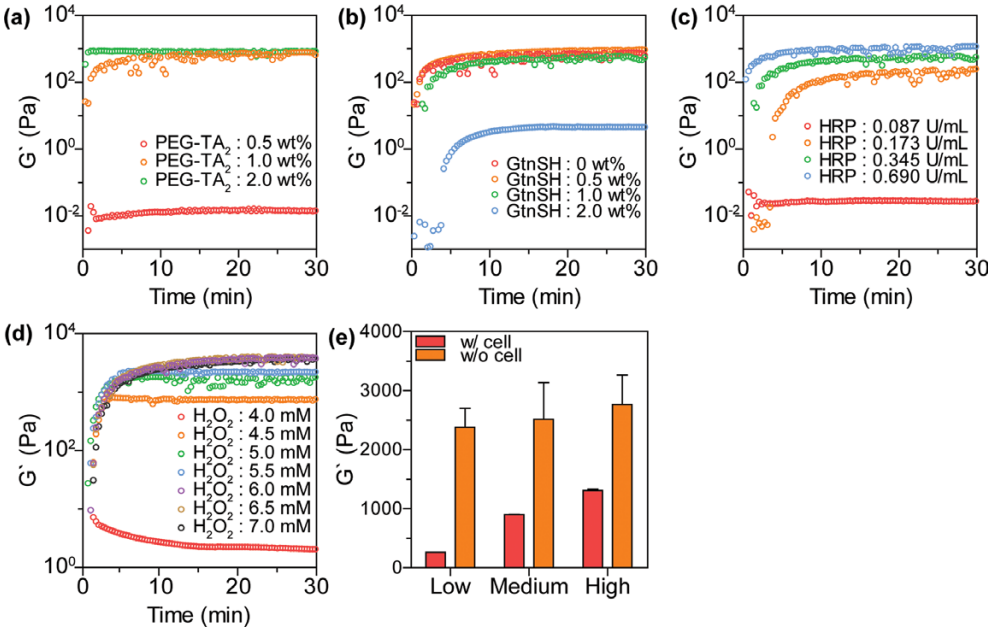

Figure 4. Tunable elastic modulus (G') of the IPN hydrogels. The effect of (a) PEG-TA_2, (b) GtnSH, (c) HRP, (d) H_2O_2, and (e) cell encapsulation on elastic modulus.

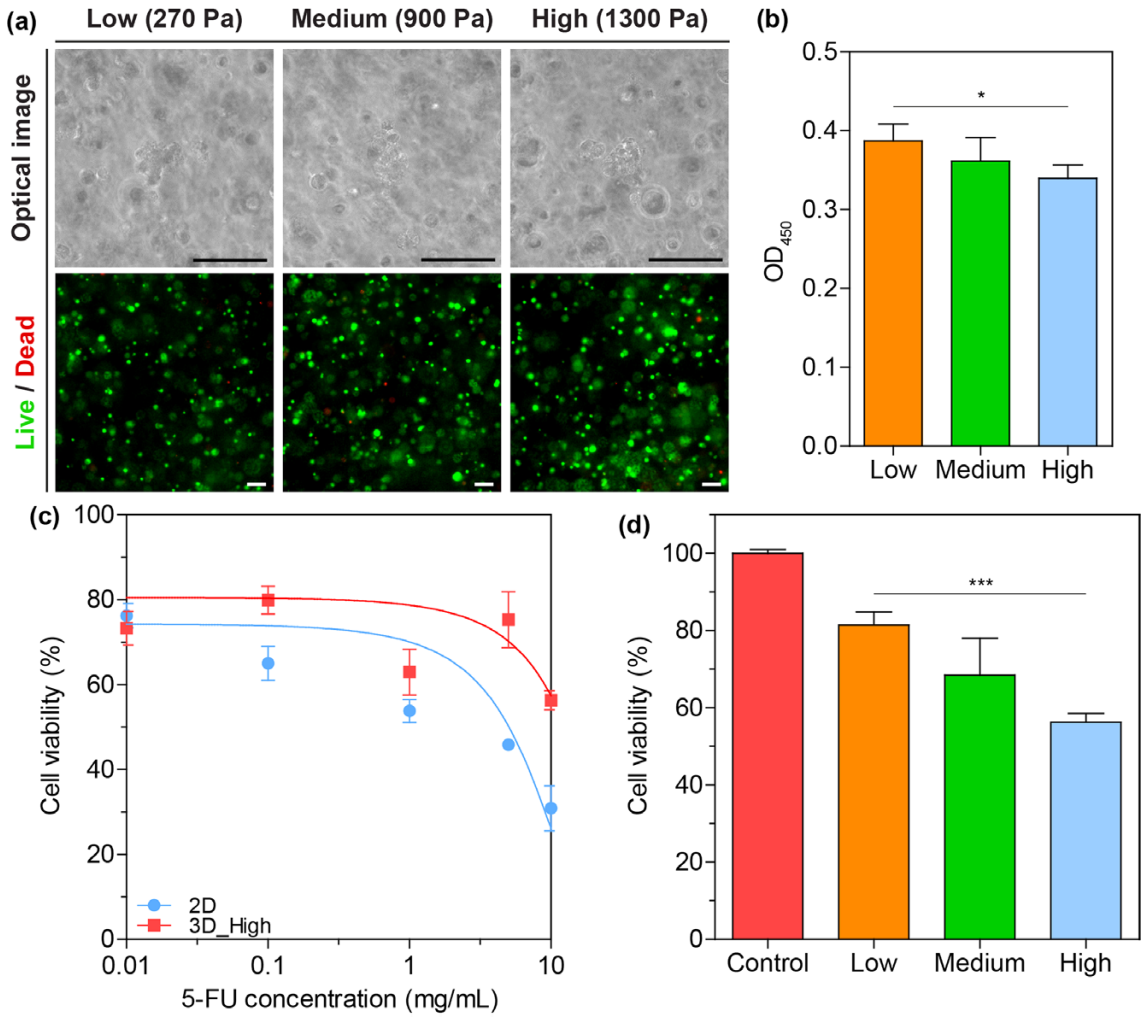

Figure 5. IPN matrices as engineered tumor microenvironments. The effect of matrix stiffness on HT1080 proliferation: (a) Optical and fluorescent images of the cells cultured within the IPN hydrogels and (b) the quantitative analysis of cell proliferation depending on the matrix stiffness. Scale bars in (a) is 100 μm. (c) Comparisons of drug resistance to 5-FU between 2D and 3D models. (d) The effect of matrix stiffness on drug resistance to 5-FU. The results in (b) and (d) are shown as the average±s.d. (n=3-4, *P<0.05 and ***P<0.001).

Medium, 900 Pa; Low, 270 Pa) and cultured them for up to seven days. We then analyzed the cell viability and proliferative activity depending on the matrix stiffness. We observed predominantly viable cells within the hydrogels without morphological changes of the cells depending on the matrix stiffness (Figure 5(a)). This result demonstrates that our IPN hydrogels provide cytocompatible matrices to create engineered tumor constructs. Interestingly, the cells cultured within the stiffer matrices showed lower proliferation compared to those within the softer ones (Figure 5(b)). The rigidity of the tumor microenvironment is known to play an essential role in regulating cancer progression and metastasis.[28-30] Although we did not investigate all mechanical strengths, we found that the soft matrices enhanced the proliferation of HT1080 cells compared to the stiff microenvironments.

Resistance to anticancer drugs is considered to be the biggest problem in the treatment of tumors.[34-37] Therefore, many researchers have endeavored to develop advanced preclinical models capable of evaluating the resistance of tumors to commercially available or newly developed anticancer drugs. We finally utilized our engineered constructs as a platform to evaluate the resistance of cells against the commercially available 5-FU, as a model anticancer drug. We first compared the drug resistance of our 3D tumor models to that of traditional 2D culture as a gold standard for cancer research. The engineered 3D tumor constructs showed higher IC50 values (12.64±3.1 mg/mL) compared to the 2D culture method (5.05±0.78 mg/mL). We then investigated the effect of matrix stiffness on drug resistance. Toward this end, we administered the drug (10 mg/mL) to the tumor constructs after one day of culture. Interestingly, the soft matrices exhibited higher drug resistance compared to that of the stiff matrices, which is consistent with the results of cell proliferation.

Taken together, we suggest that our IPN hydrogels can be utilized as an advanced platform to study basic cancer biology and identify novel therapeutic targets and newly developed anticancer drugs.

4. Conclusions

In this study, we present a new type of IPN hydrogels that can serve as engineered tumor microenvironments. The IPN hydrogels were fabricated *via* HRP-mediated dual cross-linking reactions. The gelation time and matrix stiffness could be controlled

independently by varying the concentration of HRP and H_2O_2 without changing the polymer composition. The IPN hydrogels provided cytocompatible cellular microenvironments for long-term culture of cancer cells to create engineered tumor constructs. Using advanced preclinical models, we examined the effect of the stiffness of artificial microenvironments on cancer cell proliferation and drug resistance. We suggest that our IPN hydrogel is a promising material to create engineered tumor microenvironments for a wide range of cancer research, including the study of basic cancer biology and screening of potential therapeutics for better clinical outcomes.

References

(1) M. S. Tessmer and K. T. Flaherty, *Clin. Cancer Res.*, **23**, 5325 (2017).
(2) N. E. Davidson, S. A. Armstrong, L. M. Coussens, M. R. Cruz-Correa, R. J. DeBerardinis, J. H. Doroshow, M. Foti, P. Hwu, T. W. Kensler, M. Morrow, C. G. Mulligan, W. Pao, E. A. Platz, T. J. Smith, and C. L. Willman, *Clin. Cancer Res.*, **22 Suppl 19**, S1 (2016).
(3) M. Hay, D. W. Thomas, J. L. Craighead, C. Economides, and J. Rosenthal, *Nat. Biotechnol.*, **32**, 40 (2014).
(4) M. De Palma, D. Biziato, and T. V. Petrova, *Nat. Rev. Cancer*, **17**, 457 (2017).
(5) D. F. Quail and J. A. Joyce, *Nat. Med.*, **19**, 1423 (2013).
(6) M. Kumar, S. K. Dhatwalia, and D. K. Dhawan, *Tumour. Biol.*, **37**, 14341 (2016).
(7) S. M. Weis and D. A. Cheresh, *Nat. Med.*, **17**, 1359 (2011).
(8) D. Ackerman and M. C. Simon, *Trends Cell Biol.*, **24**, 472 (2014).
(9) K. M. Park, D. Lewis, and S. Gerecht, *Annu. Rev. Biomed. Eng.*, **19**, 109 (2017).
(10) K. M. Park and S. Gerecht, *Eur. Polym. J.*, **72**, 507 (2015).
(11) S. Park and K. M. Park, *Biomaterials*, **182**, 234 (2018).
(12) K. M. Park, K. S. Ko, Y. K. Joung, H. Shin, and K. D. Park, *J. Mater. Chem.*, **21**, 13180 (2011).
(13) K. M. Park, M. R. Blatchley, and S. Gerecht, *Macromol. Rapid Commun.*, **35**, 1968 (2014).
(14) K. M. Park and S. Gerecht, *Nat. Commun.*, **5**, 4075 (2014).
(15) K. M. Park, Y. Lee, J. Y. Son, D. H. Oh, J. S. Lee, and K. D. Park, *Biomacromolecules*, **13**, 604 (2012).
(16) C. Li, C. Mu, W. Lin, and T. Ngai, *ACS Appl. Mater. Interfaces*, **7**, 18732 (2015).
(17) S. Kalia, *Polymeric Hydrogels as Smart Biomaterials*, Springer, 2016.
(18) B. J. Klotz, D. Gawlitta, A. Rosenberg, J. Malda, and F. P. W. Melchels, *Trends Biotechnol.*, **34**, 394 (2016).
(19) S. Sokic and G. Papavasiliou, *Tissue Eng. Part A*, **18**, 2477 (2012).
(20) G. P. Raeber, M. P. Lutolf, and J. A. Hubbell, *Biophys. J.*, **89**, 1374 (2005).
(21) A. M. Zaton and E. Ochoa de Aspuru, *FEBS Lett.*, **374**, 192 (1995).
(22) R. Safiri, R. H. Sajedi, and V. Jafarian, *J. Mol. Liq.*, **123**, 20 (2006).
(23) D. R. Edwards and G. Murphy, *Nature*, **394**, 527 (1998).
(24) L. M. Coussens and Z. Werb, *Nature*, **420**, 860 (2002).
(25) K. Kessenbrock, V. Plaks, and Z. Werb, *Cell*, **141**, 52 (2010).
(26) S. D. Shapiro, *Curr. Opin. Cell Biol.*, **10**, 602 (1998).
(27) H. Sato, T. Takino, Y. Okada, J. Cao, A. Shinagawa, E. Yamamoto, and M. Seiki, *Nature*, **370**, 61 (1994).
(28) S. Kumar and V. M. Weaver, *Cancer Metastasis Rev.*, **28**, 113 (2009).
(29) D. Fukumura and R. K. Jain, *J. Cell. Biochem.*, **101**, 937 (2007).
(30) P. P. Provenzano, D. R. Inman, K. W. Eliceiri, J. G. Knittel, L. Yan, C. T. Rueden, J. G. White, and P. J. Keely, *BMC Med.*, **6**, 11 (2008).
(31) E. A. Phelps, N. O. Enemchukwu, V. F. Fiore, J. C. Sy, N. Murthy, T. A. Sulchek, T. H. Barker, and A. J. Garcia, *Adv. Mater.*, **24**, 64 (2012).
(32) A. A. Starkov, A. Y. Andreyev, S. F. Zhang, N. N. Starkova, M. Korneeva, M. Syromyatnikov, and V. N. Popov, *J. Bioenerg. Biomembr.*, **46**, 471 (2014).
(33) L. Slade, J. Chalker, N. Kuksal, A. Young, D. Gardiner, and R. J. Mailloux, *Biochim. Biophys. Acta Gen. Subj.*, **1861**, 1960 (2017).
(34) M. Nikolaou, A. Pavlopoulou, A. G. Georgakilas, and E. Kyrodimos, *Clin. Exp. Metastasis*, **35**, 309 (2018).
(35) J. Rueff and A. S. Rodrigues, *Methods Mol. Biol.*, **1395**, 1 (2016).
(36) G. Housman, S. Byler, S. Heerboth, K. Lapinska, M. Longacre, N. Snyder, and S. Sarkar, *Cancers (Basel)*, **6**, 1769 (2014).
(37) P. Periti and E. Mini, *J. Chemother.*, **1**, 5 (1989).

